J Mater Sci: Mater Med (2015) 26:238
DOI 10.1007/s10856-015-5579-z

BIOCOMPATIBILITY STUDIES

Original Research

Improvement of bioactivity, degradability, and cytocompatibility of biocement by addition of mesoporous magnesium silicate into sodium-magnesium phosphate cement

Yingyang Wu[1] · Xiaofeng Tang[1] · Jie Chen[1] · Tingting Tang[2] · Han Guo[3] · Songchao Tang[1] · Liming Zhao[1] · Xuhui Ma[4] · Hua Hong[1] · Jie Wei[1]

Received: 3 May 2015 / Accepted: 18 September 2015 / Published online: 22 September 2015

Abstract A novel mesoporous magnesium-based cement (MBC) was fabricated by using the mixed powders of magnesium oxide, sodium dihydrogen phosphate, and mesoporous magnesium silicate (m-MS). The results indicate that the setting time and water absorption of the MBC increased as a function of increasing m-MS content, while compressive strength decreased. In addition, the degradability of the MBC in a solution of Tris–HCl and the ability of apatite formation on the MBC were significantly improved with the increase in m-MS content. In cell culture experiments, the results show that the attachment, proliferation, and alkaline phosphatase activity of the MC3T3-E1 cells on the MBC were significantly enhanced with the increase of the content of m-MS. It can be suggested that the MBC with good cytocompatibility could promote the proliferation and differentiation of the MC3T3-E1 cells. In short, our findings indicate that the MBC containing m-MS had promising potential as a new biocement for bone regeneration and repair applications.

✉ Hua Hong
biomaterbone@163.com

✉ Jie Wei
jiewei7860@sina.com

Yingyang Wu
13262918095@163.com

[1] Key Laboratory for Ultrafine Materials of Ministry of Education, East China University of Science and Technology, Shanghai 200237, People's Republic of China

[2] Shanghai Key Laboratory of Orthopaedic Implants, Department of Orthopaedic Surgery, Shanghai Ninth People's Hospital, Shanghai Jiaotong University School of Medicine, Shanghai 200011, People's Republic of China

[3] Shanghai Synchrotron Radiation Facility, Shanghai Institute of Applied Physics, Chinese Academy of Sciences, Shanghai 201800, People's Republic of China

[4] Polymer Science (Shenzhen) New Materials Co., Ltd., Shenzhen 518101, People's Republic of China

1 Introduction

Calcium (Ca)-containing biomaterials, such as calcium sulfate, calcium phosphate, and calcium silicate, are traditionally inorganic bioactive materials, which have been widely used for bone tissue regeneration [1, 2]. Magnesium (Mg) is the fourth most abundant cation in the human body and is commonly found in bone [3]. It is known that magnesium can influence bone mineral metabolism, bone formation, and crystallization processes [4]. In previous work, magnesium phosphate cement (MPC) has been reported to be a kind of bone cement for bone regeneration [5]. The main components of MPC are the mixed powders containing sintered magnesia (MgO) and ammonium dihydrogen phosphate ($NH_4H_2PO_4$), which when reacted with water form ammonium magnesium phosphate (NH_4MgPO_4) as the final product [6, 7]. MPC is a kind of bioactive bone cement with the characteristics of rapid setting and early-high compressive strength, and can induce apatite layers on its surface [8, 9]. It has also been reported that the MPC was degradable, releasing the magnesium ion to improve the activity of the osteoblasts after implantation in vivo [10]. However, the final product of ammonium magnesium phosphate containing an NH_4 group would release NH_3 in the physiological environment, generating cytocompatibility issues [11]. Therefore, novel bioactive bone cements should be developed for bone regenerations.

Mesoporous materials have received enormous attention owing to their potential applications in catalysis, separation, biomaterials, and drug release [12]. Recently, the use of

mesoporous materials for bone regeneration has been proposed because their large surface area and pore volume may enhance their bioactive behaviors and promote new bone formation [13, 14]. A previous study has showed that mesoporous magnesium silicate (m-MS) with high specific surface area and pore volume showed excellent bioactivity, water absorption, and degradability in applications of bone regeneration biomaterials [15]. Considering the disadvantages and advantages of MPC and m-MS, in this study, a novel mesoporous magnesium-based cement (MBC) was developed by using the mixture of magnesium oxide (MgO), sodium dihydrogen phosphate ($NaH_2PO_4{\cdot}H_2O$), and m-MS as cement powders and water as cement liquid. It is expected that the setting time, compressive strength, water absorption, in vitro bioactivity and degradability, and primary cytocompatibility of the novel MBC would be improved by addition of m-MS into magnesium-based cements. Moreover, it is thought that the MBC may have promise as a new biocement for bone repair.

2 Materials and methods

2.1 Preparation of m-MS

The m-MS was prepared as follows: Pluronic P123 ($EO_{20}PO_{70}EO_{20}$, m.w., 5800) and 5 % (v/v) hydrochloric acid was dissolved in water under constant stirring until a clear solution was obtained. Thereafter, 9.4 g magnesium nitrate hexahydrate was added to the solution, followed by the addition of 16.9 g of tetraethyl orthosilicate at 60 °C for 24 h. The acquired white suspension was washed thoroughly with deionized water and then dried at 100 °C in an oven to obtain the powder. Finally, the m-MS product was obtained by calcining at 650 °C for 6 h at a heating rate of 1 °C/min [16]. All chemicals used were purchased from Sigma Chemical Reagent Co. Ltd.

2.2 Preparation of MBC

The MgO was prepared in a furnace by heating magnesium carbonate pentahydrate at 1500 °C for 6 h [17]. The mesoporous magnesium-based cement (MBC) paste without m-MS (MBC0), and MBC with 15 w % (MBC15) and 30 w % (MBC30) were fabricated by mixing the cement powders (containing MgO, $NaH_2PO_4{\cdot}H_2O$, and m-MS) and water, in which the MgO and $NaH_2PO_4{\cdot}H_2O$ was of a molar ratio of 1:1. The MBC paste was placed within a tetrafluoroethylene mould (Φ12 × 3 mm) and subjected to a pressure of 0.2 MPa. The hardened cements were stored in disposable cups in an oven at 37 °C and 100 % relative humidity for 5 days. The prepared MBC samples were characterized by Fourier transform-infrared spectroscopy (FT-IR; Magna-IR 550, Nicolet) and X-ray diffraction (XRD; Rigaku Co., Japan). All the chemicals used were purchased from Sigma Chemical Reagent Co. Ltd.

2.3 Setting time, compressive strength, and water absorption of MBC

The setting time of the cement samples (MBC0, MBC15, and MBC30) was tested by using a Vicat apparatus bearing a 300-g needle, 1 mm in diameter. Each cement sample was placed in a cylindrical mold. The setting time was recorded as the time elapsed between the end of mixing and the time when the needle failed to create an indentation of 1 mm in depth in three separate areas of the cement [18].

The compressive strength of the cement samples (MBC0, MBC15, and MBC30) was measured using a universal testing machine (AG-2000A, Shimadzu Autograph, Shimadzu Co. Ltd., Japan) at a loading rate of 1 mm min^{-1}.

The water absorption of the MBCs was tested using deionized water. A known amount of dried MBC was dipped into a Petri dish with 20 mL water for 1 min and then the samples were extracted from the water. Afterwards, the surface of the wetted samples was gently wiped and the weight was measured. The water absorption was calculated by using the following equation:

$$\text{water absorption } (\%) = \frac{W_{\text{wet}} - W_0}{W_0} \times 100$$

where W_{wet} is the weight of the wet materials and W_0 is the weight of the dry materials.

2.4 In vitro degradation of MBC in Tris–HCl solution

The cement samples (MBC0, MBC15, and MBC30) weighing ~0.2 g were placed in plastic bottles filled with 40 mL Tris–HCl solution (pH 7.40). The bottles with samples were placed in a shaking box at 37 °C (100 rpm/min) for 12 weeks, replacing the solution once a week.

At specific time intervals (1, 2, 3, 4, 5, 6, 7, 8, 9, 10, 11, and 12 weeks), the samples were washed with deionized water thoroughly and then dried at 100 °C in an oven for 24 h. The weight loss ratio of the cement samples was determined according to the following equation:

$$\text{weight loss } (\%) = \frac{W_t - W_0}{W_0} \times 100$$

where W_0 is the starting weight and W_t is the weight of the samples at time t. In addition, the pH value of the solutions at the specific time intervals was tested using a pH meter (PHS-2C; Jingke Leici, Shanghai, China).

2.5 In vitro bioactivity of MBC in a simulated body fluid (SBF)

The in vitro bioactivity of the cement samples (MBC0, MBC15, and MBC30) was characterized by testing the apatite formation on the samples surface. The specimens were soaked in a SBF (pH 7.40) at 37 °C for varying times. The samples were placed into plastic bottles filled with 40 mL SBF solution. The bottles with samples were placed in a shaking box at 37 °C (100 rpm/min) for different times. At each specific time interval (1, 3, 5, and 7 days), the samples were washed with deionized water thoroughly and then dried at 100 °C in an oven for 24 h.

The concentrations of Ca, Mg, Si, and P ions in the SBF solution at the selected times were analyzed by inductively coupled plasma-atomic emission spectroscopy (ICP-AES; IRIS 1000, Thermo Elemental, USA), and the pH values of the solutions at the respective times determined by a pH meter (PHS-2C, JingkeLeici, Shanghai, China). The phase surface morphology and composition of the samples were characterized by scanning electron microscopy (SEM; S-3400 N, Hitachi, Japan) and energy dispersive spectroscopy (EDS, Falcon, USA), respectively.

2.6 Cell culture

MC3T3-E1 cells were used to evaluate the cytocompatibility of the cement samples. The cells were maintained with 5 % CO_2 at 37 °C in Dulbecco's Modified Eagle's Medium. The culture medium was supplemented with 10 % (v/v) fetal calf serum (Sijiqing, Hangzhou, China) and 1 % (v/v) antibiotics. The culture medium was replaced every 2 days. The trypsin-DETA solution (Gibco, 0.5 g/L and 0.2 g/L, respectively) was used to harvest cells before cells reached confluence. The cells were resuspended in fresh culture medium before seeding on specimens.

2.6.1 Cell proliferation

The proliferation of the MC3T3-E1 cells on the samples was determined using a cell counting Kit 8(CCK-8) at 1, 3, and 7 days. The cells were seeded on the specimens in 24-well plates at a concentration of 1×10^4 cells/50 mL. The plates were incubated at 37 °C under an atmosphere of 100 % humidity with 5 % CO_2 in the culture medium and the medium was replaced every 2 days. At the specific time point, the specimens were gently rinsed three times with phosphate buffered saline (PBS), transferred to a new 24-well plate and 10 μL CCK-8 solution (Dojindo Molecular Technologies Inc., Japan) added to each well. Thereafter, the plates were incubated in the cell culture incubator for 3 h and subsequently 100 μL of the supernatant was transferred into a new 24-well plate. Cell proliferation was followed by electronic cell counting using a microplate reader (Synergy HT, Bio-tek, USA).

2.6.2 Cell morphology

The MC3T3-E1 cells were seeded on the samples in a 24-well plate under 100 % humidity at 37 °C with 5 % CO_2. After the cells cultured for 1, 3, and 7 days, the specimens were carefully washed three times with PBS to remove any unattached cells. The samples cleaned with PBS were fixed in a 4 % paraformaldehyde solution for 16 min. After washing with PBS, the rest of the cells were incubated with FITC-Phalloidin (Cytoskeleton Inc., USA) for 45 min and then counterstained with DAPI (Beyotime Institute of Biotechnology, China) for 8 min to observe the nucleus. The cell morphology was visualized using confocal laser scanning microscopy (Nikon A1R, Japan).

2.6.3 Alkaline phosphatase activity (ALP)

The MC3T3-E1 cells (2.5×10^4) were seeded on the samples, which were then placed in 24-well plates followed by culturing under 100 % humidity at 37 °C with 5 % CO_2. At the specific time point, the culture medium was removed and the cells were washed. To obtained cell lysates, 1 mL of 0.2 % Nonidet P-40 solution (NP-40) was added to each well at room temperature for 1 h. Thereafter, 50 μL of 1 mg/mL p-nitrophenylphosphate (Sigma, USA) substrate solution (pH 9, containing 0.1 mol/L glycine and 0.5 mmol/L $MgCl_2$ in 1 M diethanolamine buffer) was added to each well and incubated at 37 °C for 16 min. Finally, the reaction was stopped by 100 μL of 0.1 M sodium hydroxide. The OD value was measured using a microplate reader (SPECTR Amax 384, Molecular Devices, USA) at a wavelength of 405 nm. The ALP activity was expressed as the OD value per total protein content. The total protein content was measured using the BCA protein assay kits and a series of bovine serum albumin standards.

2.7 Statistical analysis

All quantitative data were analyzed with Origin 8.0 (Origin Lab Corporation, USA) and expressed as the mean ± standard deviation (M ± SD). For all cell experiments, the data encompassed repeat statistics ($n = 5$). To compare the data, statistical credibility was over a 95 % confidence level ($P < 0.05$).

3 Results

3.1 Characterization of MBC

Figure 1 shows the IR spectra of the MBC0, MBC15, and MBC30 samples. The absorption bands at 1070 and 950 cm^{-1} were ascribed to PO_4^{3-}. The peaks at 1750 cm^{-1} and the broad band ranging from 2800 to 3472 cm^{-1} were attributed to the absorbed water. The band at 872 cm^{-1} may correspond to the vibration of P–O–H from $NaH_2PO_4{\cdot}H_2O$ [19]. The peak at around 800 cm^{-1} was attributed to SiO_3^{2-} [20], which was present on MBC15 and MBC30; however, on MBC0 this peak was absent. The peak corresponding to SiO_3^{2-} was more profound in the MBC with increased levels of m-MS.

Figure 2 shows the XRD of the MBC0, MBC15, and MBC30 materials. It is discernable that the MBC containing the main hydration product of MBC0 was sodium magnesium phosphate ($NaMgPO_4$) [21], and both MBC15 and MBC30 contained $NaMgPO_4$ and m-MS. The diffraction intensity of sodium-magnesium phosphate decreased with increasing m-MS content.

3.2 Setting time, compressive strength, and water absorption

Table 1 shows the setting time and compressive strength of MBC0, MBC15, and MBC30. It was found that the setting time of MBC0 was 10 min while the setting time of MBC15 and MBC30 were 12 min and 14 min, respectively. In addition, it is found that the compressive strength of MBC0 reached 5.5 MPa while the compressive strength of MBC15 and MBC30 was 3.1 and 2.8 MPa, respectively. Figure 3 shows the water absorption of MBC0, MBC15, and MBC30. It can be seen that the water absorption of MBC0, MBC15 and MBC30 was 72.2, 80.3 and 87.5 % after soaked into deionized water for 1 min, indicating that the water absorption of MBC increased with the increase of m-MS content.

3.3 Degradation in Tris–HCl solution

Figure 4 shows the weight loss ratio of MBC0, MBC15, and MBC30 after immersing in Tris–HCl solution for specific times. It is found that the weight loss ratio of MBC

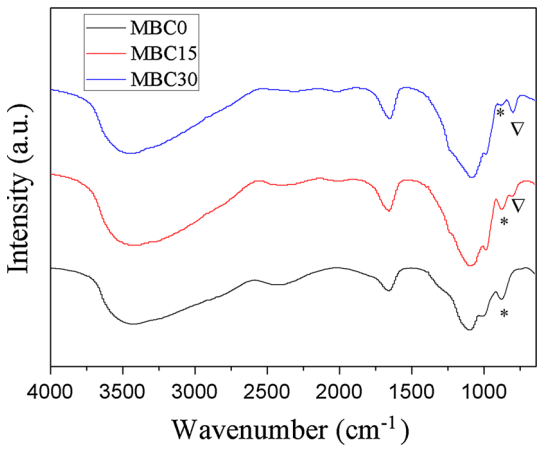

Fig. 1 IR of MBC0, MBC15 and MBC30 after setting for 7 days; *asterisks* represent $NaMgPO_4$; *inverted triangle* represent SiO_3^{2-}

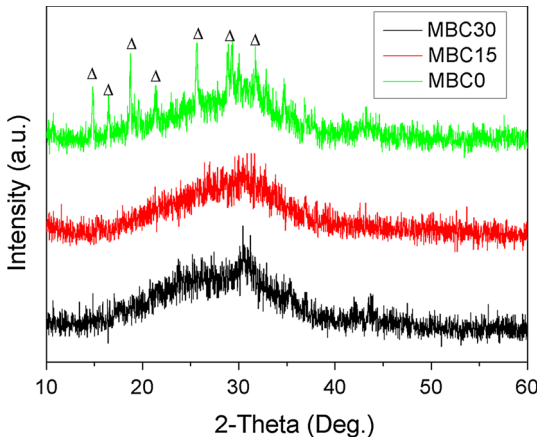

Fig. 2 XRD of MBC0, MBC15 and MBC30 after setting for 7 days; *triangle* represent $NaMgPO_4$

Table 1 Setting time and compressive strength properties of the MBC

Samples	Setting time (min)	Compressive strength (MPa)
MBC0	10.0 ± 0.5	5.5 ± 1
MBC15	12.0 ± 0.5	3.1 ± 2
MBC30	14.0 ± 0.5	2.8 ± 1

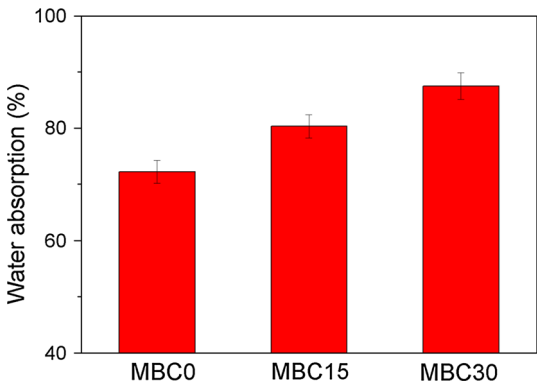

Fig. 3 Water absorption of MBC0, MBC15 and MBC30 after immersed in deionized water for 1 min

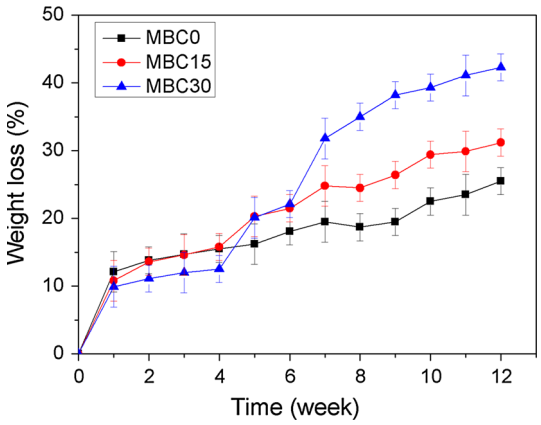

Fig. 4 Weight loss of MBC0, MBC15 and MBC30 after immersed in Tris–HCl solution for different time

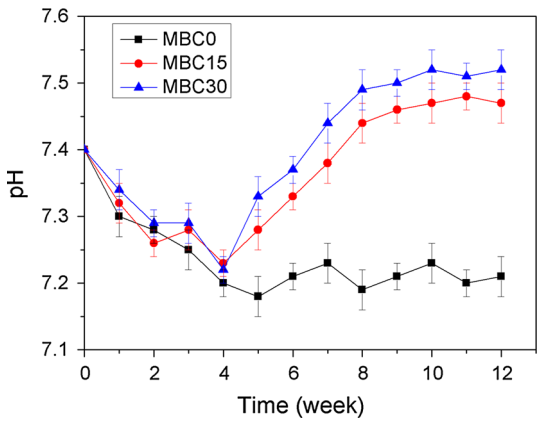

Fig. 5 Change in pH of Tris–HCl solution after MBC0, MBC15 and MBC30 immersed into solution for 12 weeks

increased with increasing m-MS content, and MBC30 had the greatest weight loss ratio among these samples. It was found that the weight loss ratio of MBC30 was 42.3 wt% after being immersed into the Tris–HCl solution for 12 weeks, which was higher than MBC15 of 31.2 wt% and MBC0 of 25.5 wt%.

Figure 5 presents the pH change of the solution after MBC0, MBC15, and MBC30 were soaked into the Tris–HCl solution at varying times. It was observed that the pH of the solution for MBC0 decreased from the initial value of 7.40–7.20 during 12 weeks of soaking time, while the pH for MBC15 and MBC30 at the first 4 weeks decreased from 7.40 to around 7.22 and then increased from 7.22 to 7.47/7.52 (from 4 to 12 weeks). Furthermore, the pH of the solution for MBC30 was slightly higher than the corresponding MBC15, and obviously higher than MBC0.

Figure 6 shows the SEM micrographs of the surface morphology of MBC after immersion in Tris–HCl solution for 8 weeks. It can be seen that the degradation of the MBC30 (Fig. 6c) was faster and presented frequent deep cracks on its surface. However, for the MBC15 sample (Fig. 6b), several small cracks could be observed, while for MBC0 (Fig. 6a), no obvious cracks were observed. In addition, under high magnification conditions, an abundance of small pores were evident on the surface of the three samples (Fig. 6d–f), and the pores size of MBC increased with the increase of m-MS content, which might increase the surface area of the samples and accelerate the dissolution process.

3.4 In vitro bioactivity of MBC in SBF

Figure 7a–c show the SEM micrographs of the surface morphology of MBC0, MBC15, and MBC30 after being immersed into SBF for 7 days. It was observed that the surface of three samples presented apatite coverage of spherical shape. In addition, the apatite on the MBC30 surface was obviously higher in concentration than MBC15 and MBC0. Figure 7d–f show the EDS of the surfaces of MBC0, MBC15, and MBC30 after being soaked in SBF for 7 days. P and Ca peaks appeared visibly after immersion into SBF for 7 days. Figure 8 shows the XRD of MBC0, MBC15, and MBC30 after soaking in SBF for 7 days. The results show that two peaks appear at 26° and 32°, indicating that the apatite phase was present on the MBC surfaces.

Figure 9 shows the changes of ion concentrations of Si, Mg, P, and Ca in solution after the MBC was soaked into SBF for 0, 1, 3, 5, and 7 days. It is easily discernable that the Si and Mg ion concentrations increased as a function of time, while the Ca ion concentration slowly decreased. In addition, the P ion concentration increased during the first 12 h and then gradually decreased to 3 days, thereafter, the P ion concentration slowly increased to 7 days.

3.5 In vitro cytocompatibility

3.5.1 Cell proliferation and morphology

The proliferation of the MC3T3-E1 cells on MBC0, MBC15, and MBC30 is shown in Fig. 10. It can be seen that the OD value for all the samples increased with culture time, indicating good cytocompatibility. No obvious differences of the OD value were found for all samples at 1 and 3 days, while the OD value for MBC15 and MBC30 was significantly higher than MBC0 at 7 days.

The morphology of the MC3T3-E1 cells seeded on the MBC is shown in Fig. 11. It is evident that the MC3T3-E1 cells exhibited a spindled appearance spread on the MBC0, MBC15, and MBC30 surfaces. In addition, it was found that the morphology and spreading of the cells were optimum upon increased m-MS content (the cells' spread is more enhanced on the MBC30 surface than the corresponding MBC15 and MBC0 materials).

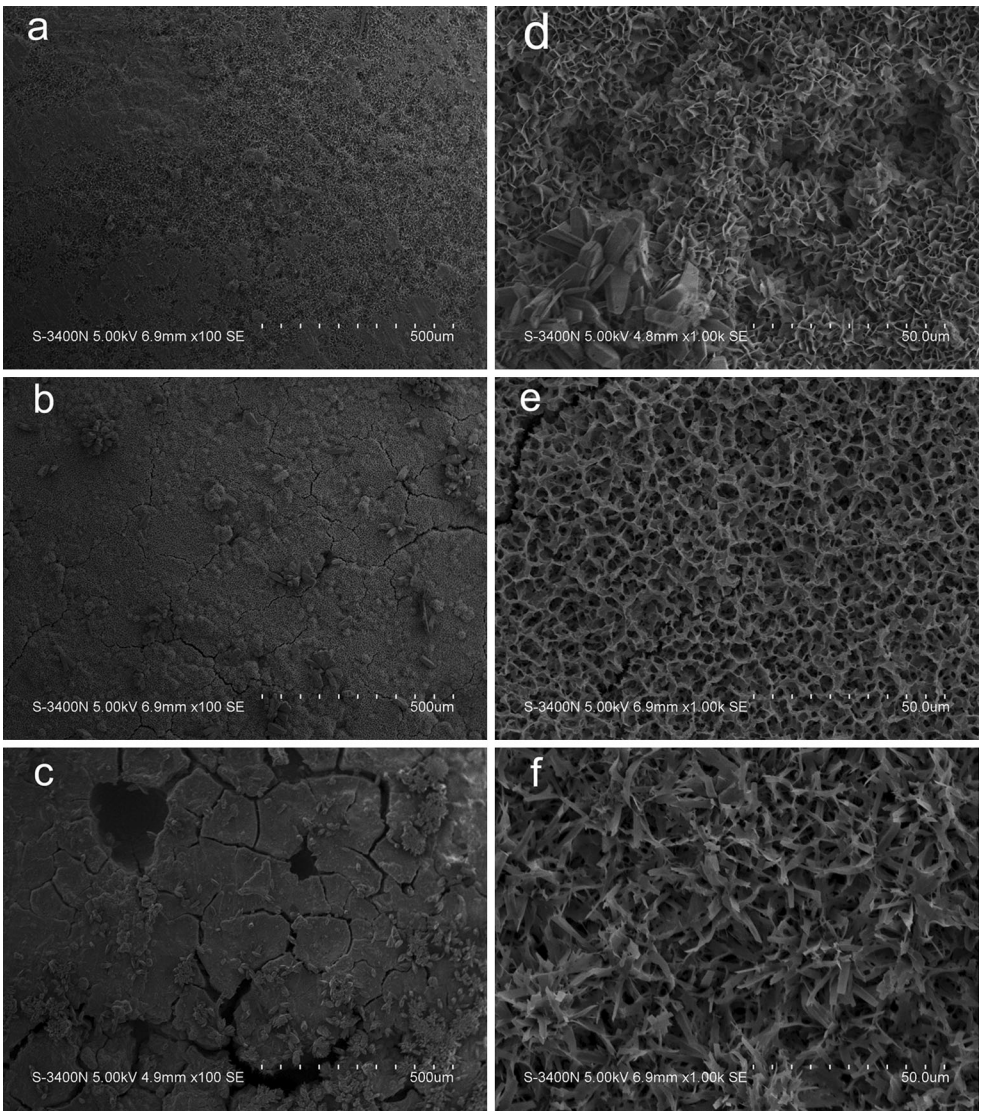

Fig. 6 SEM images of the morphology/microstructure of MBC0 (**a** and **d**), MBC15 (**b** and **e**) and MBC30 (**c** and **f**) under different magnifications after immersion in Tris–HCl solution for 8 weeks

3.5.2 Alkaline phosphatase activity (ALP)

Figure 12 shows the ALP activity of MC3T3-E1 cells cultivated on MBC0, MBC15, and MBC30 at 4, 7, and 14 days. It was found that the ALP activity of the cells increased as a function of time for the three samples, indicating good cytocompatibility. In addition, no significant difference of ALP activity was found for all the samples at 4 and 7 days, while the ALP activity of the cells on MBC30 and MBC15 was significantly higher than MBC0 at 14 days, indicating that the MC3T3-E1 cells differentiated most at 14 days.

4 Discussions

In this study, a novel mesoporous magnesium-based cement (MBC) was fabricated by using the mixed powders of magnesium oxide (MgO), sodium dihydrogen phosphate (NaH_2PO_4), and mesoporous magnesium silicate (m-MS). The results from IR and XRD show that the MBC containing the main hydration product of MBC0 was sodium-magnesium phosphate ($NaMgPO_4$), and both MBC15 and MBC30 contained $NaMgPO_4$ and m-MS. The final hardened product of MBC0 was $NaMgPO_4$, which were attributed to the acid–base reaction of magnesium oxide

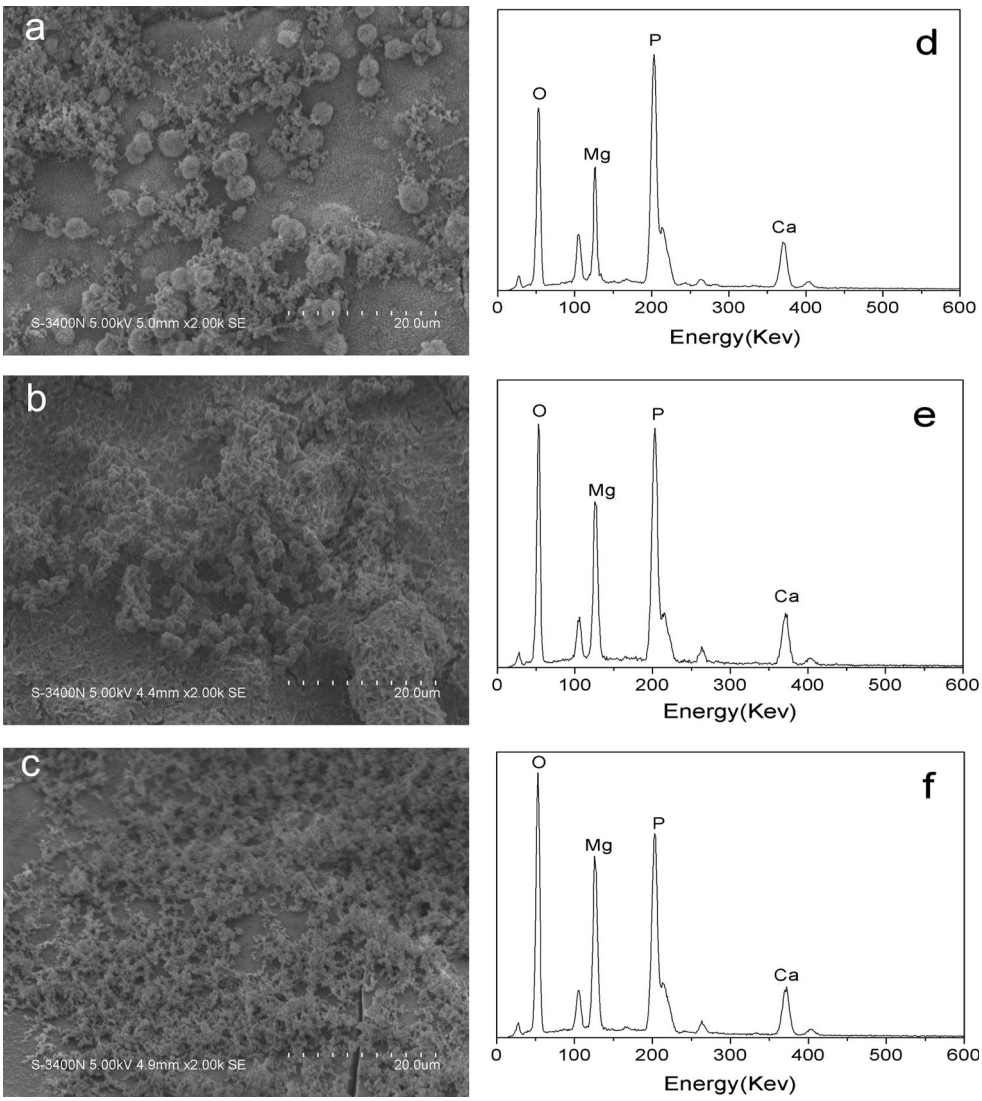

Fig. 7 SEM images of surface morphology and EDS of MBC0 (**a** and **d**), MBC15 (**b** and **e**) and MBC30 (**c** and **f**) soaked into SBF for 7 days

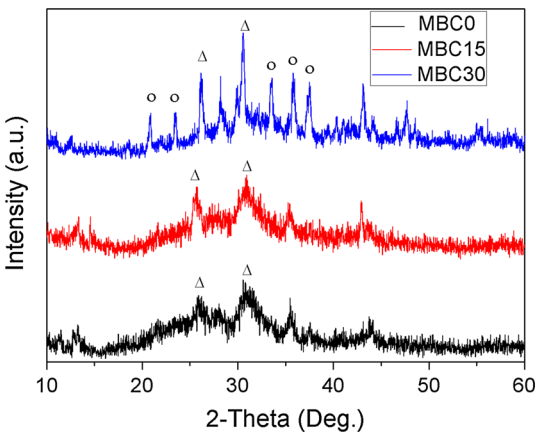

Fig. 8 XRD of MBC0, MBC15 and MBC30 after immersed into SBF for 7 days; *triangle* represent apatite; *open circle* represent $NaMgPO_4$

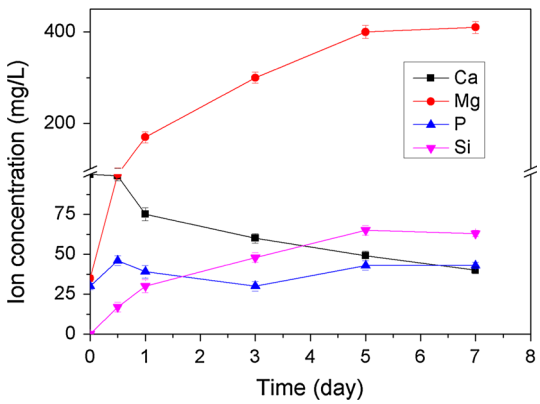

Fig. 9 Changes of ion concentrations in solution after MBC30 immersed into SBF for different periods

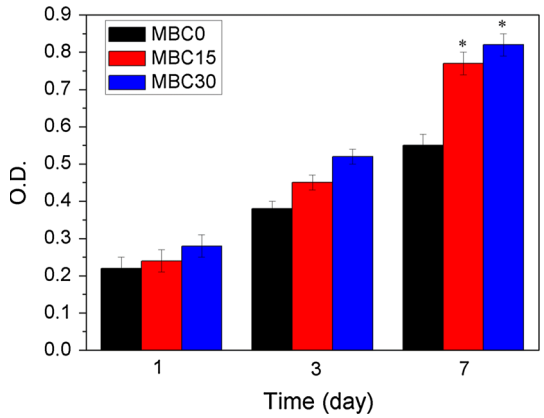

Fig. 10 Cell proliferation on MBC0, MBC15 and MBC30 at 1, 3 and 7 days (*$P < 0.05$)

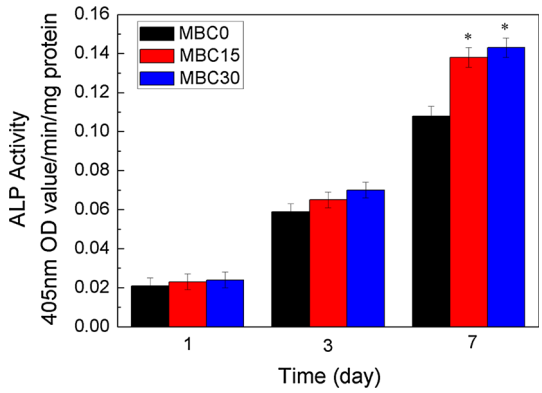

Fig. 12 ALP activity of MC3TS-E1 cells on MBC0, MBC15 and MBC30 at 4, 7and 14 days (*$P < 0.05$)

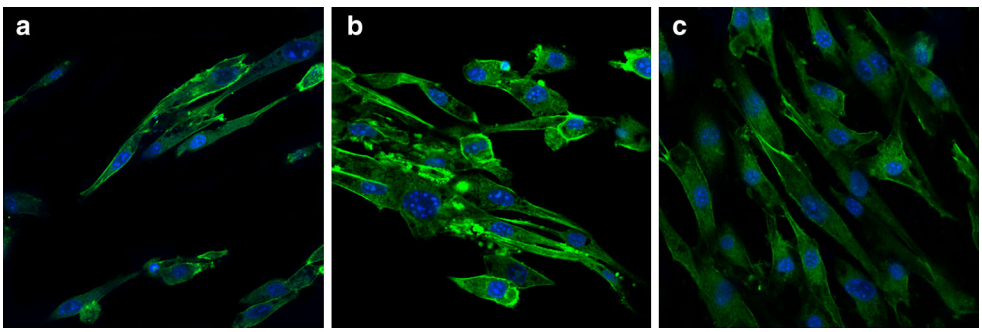

Fig. 11 Photos (confocal laser scanning microscopy) of cytoskeletal morphology and spreading of MC3TS-E1cells on MBC0, MBC15 and MBC30 at 3 days

and sodium dihydrogen phosphate ($MgO + NaH_2PO_4 \rightarrow NaMgPO_4$). Therefore, the final hardened products of MBC15 and MBC30 were sodium magnesium phosphate ($NaMgPO_4$) containing 15 and 30 wt% m-MS content ($NaMgPO_4$ + m-MS).

The setting time and compression strength are very important for bone cement, and in surgical operations, 12–15 min is sufficient for a surgeon to mix the bone cement and place the cement paste in the bone defects [8, 22]. In this study, the results show that the setting time of MBC15 and MBC30 were 12 and 14 min, and the setting time of MBC increased with the increase of m-MS content (MBC30 > MBC15 > MBC0). In addition, the compressive strength of the MBC decreased with the increase in m-MS content, indicating that the m-MS content affected the characteristics of the MBC, such as setting time and mechanical strength.

A previous study has shown that the incorporation of mesopores into MS resulted in a remarkable increase in water absorption for m-MS, indicating that the greater specific surface area and pore volume of m-MS enhanced its capacity to absorb water [15]. In this study, the results show that the water absorption of MBC increased with the increase of m-MS content, indicating that addition of m-MS into the cement significantly improved the water absorption of the MBC. It can be suggested that the incorporation of m-MS with high surface area and pore volume into MBC was a feasible method to improve the water absorption of the cement.

It is accepted that the biomaterials used for bone regeneration should be degradable and gradually replaced by newly formed bone tissue [23, 24]. However, previous studies have shown that the degradation rate of calcium phosphate cement was slow both in vivo and in vitro [25, 26]. In this study, the results suggest that addition of m-MS into MBC improved the degradability, and the degradation ratio of the cement increased with the increase of m-MS content. The m-MS with high surface area and pore volume, lead to more water being absorbed in the cement, which increased degradability of the MBC [15]. It can be drawn that the m-MS content could affect the degradability of MBC, which is an important property in bone repair applications.

Our finding show that the pH of the solution for MBC0 decreased from the initial value of 7.40 to 7.20 while the

pH for MBC15 and MBC30 slightly increased from 7.4 to 7.47/7.52 during 12 weeks of soaking time. Furthermore, the pH of the solution for MBC30 was slightly higher than the corresponding MBC15, and obviously higher than MBC0. The results indicate that the addition of m-MS into MBC0 significantly changed the pH of the solution. The m-MS is a silicate, which is an alkaline substance; when m-MS is soaked into water, it results in a slight increase of the pH of the solution. Therefore, the pH of the solution slightly increased when these cements containing m-MS were immersed into water (pH of solution: MBC30 > MBC15 > MBC0).

The in vitro bioactivity of the biomaterials can be evaluated by the ability of induced apatite formation, which can predict the in vivo bone bioactivity [27, 28]. In this study, the results from SEM, EDS and XRD show that the MBC could induce apatite formation on their surface in SBF for 7 days, and further apatite formation on the MBC surface was noted with increasing m-MS content, indicating that addition m-MS into the cement improved the ability of apatite formation on MBC. According to the mechanism of apatite formation of bioactive materials, it is suggested that the process of apatite precipitation on the materials was most likely dependent on the dissolution velocity and ion deposition rate on the surface of the samples [29]. Therefore, the incorporation of m-MS into MBC may prove to be a more effective method to prepare bioactive materials.

The in vitro cell culture experiments provide insight for biological evaluation of biomaterials [30]. In this study, the results show that MBC30 and MBC15 enhanced stimulated cell proliferation than the corresponding MBC0 material, indicating that incorporation of m-MS into MBC could promote cellular proliferation. In addition, the MC3T3-E1 cells with normal morphology spread on the MBC surfaces, indicating that the samples exhibited no negative effects on cell morphology or viability. Furthermore, the morphology and spreading of the cells were optimum upon increased m-MS content, indicating that the addition of m-MS into MBC was favorable for cell adhesion and proliferation, indicating good biocompatibility.

The cellular responses to biomaterials, such as growth and proliferation, depend not only on surface physical morphology but also on surface chemical compositions of the biomaterials [31]. In this study, the m-MS with high specific surface area and pore volume was added into MBC, which might provide a greater opportunity for the interaction between the cells and substrates, facilitating cell growth and proliferation. Furthermore, the different surface chemical compositions play a crucial role in determining cell responses, which is relevant to the concentration of ions released from the biomaterials (such as Ca, Si, and Mg) and the consequent cell–material interactions. It is likely that the ions released from m-MS in MBC enhanced cell proliferation.

ALP activity is an important indicator of osteoblast differentiation during in vitro experiments [32]. In this study, the results reveal that the ALP activity of the cells increased as a function of time for the three samples, indicating good cytocompatibility. Moreover, the ALP activity of the MC3T3-E1 cells on MBC30 and MBC15 exhibited higher levels of expression than on MBC0 a 14 days, indicating that incorporation m-MS into MBC could improve the cell differentiation.

It has been reported that ion-dissolution products containing Ca, Si, and Mg from bioactive materials such as bioglass/ceramics could stimulate osteoblast proliferation, differentiation, and gene expression [33, 34]. Moreover, a study has revealed the positive stimulatory effect of extracellular Ca, Si, and Mg ions from the dissolution of akermanite ($Ca_2MgSi_2O_7$) at a certain concentration range on osteoblast-like cells [35]. Therefore, in this study, the continuous dissolution of MBC under physiological conditions would produce a Ca-, Mg-, and Si-rich environment that may be responsible for stimulating cell growth, proliferation, and differentiation.

5 Conclusions

A novel mesoporous MBC was fabricated by using a mixture of MgO, $NaH_2PO_4{\cdot}H_2O$, and m-MS as cement powders and water as cement liquid. The setting time of MBC increased while compressive strength decreased with the increase of m-MS content, while the water absorption and degradability of MBC increased as a function of increasing m-MS content. The proliferation of MC3T3-E1cells on MBC15 and MBC30 was significantly enhanced when compared with MBC0, revealing excellent biocompatibility. In addition, the ALP activity of MC3T3-E1 cells expressed significantly higher levels on MBC15 and MBC30 than on MBC0 at 14 days, revealing that the MBC30 facilitated cell differentiation. The results suggest that the addition of m-MS could improve MBC degradability, bioactivity, and biocompatibility, which is promising for bioactive materials in bone regeneration applications.

Acknowledgments This study was supported by grants from the National Natural Science Foundation of China (31271031, 51173041), the International Cooperation Project of the Ministry of Science and Technology of China (2013DFB50280), the National High Technology Research & Development Program of China (863 Program) (2014AA021202), the Major International Joint Research Project between China and Korea (81461148033, 31311140253) and Special Program of Strategic Emerging Industries Development of Shenzhen (CXZZ2012070355537097).

References

1. Tanaka M, Takemoto M, Fujibayashi S, Kawai T, Tsukanaka M, Takami K, Motojima S, Inoue H, Nakamura T, Matsuda S. Development of a novel calcium phosphate cement composed mainly of calcium sodium phosphate with high osteoconductivity. J Mater Sci Mater M. 2014;25:1505–17.
2. Vlad MD, Gomez S, Barraco M. Effect of the calcium to phosphorus ratio on the setting properties of calcium phosphate bone cements. J Mater Sci Mater M. 2012;23:2081–90.
3. Christel T, Christ S, Barralet JE, Groll J, Gbureck U. Chelate bonding mechanism in a novel magnesium phosphate bone cement. J Am Ceram Soc. 2015;98:694–7.
4. Vorndran E, Ewald A, Muller F, Zorn K, Kufner A, Gbureck U. Formation and properties of magnesium–ammonium–phosphate hexahydrate biocements in the Ca–Mg–PO_4 system. J Mater Sci Mater M. 2011;22:429–36.
5. Wang AJ, Zhang J, Li JM, Ma AB, Liu LT. Effect of liquid-to-solid ratios on the properties of magnesium phosphate chemically bonded ceramics. Mater Sci Eng C. 2013;11:2508–12.
6. Masuda T, Ogino I, Mukai SR. Optimizing the dimensions of magnesium ammonium phosphate to maximize its ammonia uptake ability. Adv Powder Technol. 2013;24:520–4.
7. Liu Y, Kumar S, Kwag J, Ra C. Magnesium ammonium phosphate formation, recovery and its application as valuable resources: a review. J Chem Technol Biotechnol. 2013;88:181–9.
8. Mestres G, Ginebra M. Novel magnesium phosphate cements with high early strength and antibacterial properties. Acta Biomater. 2011;7:1853–61.
9. Wang A, Yuan Z, Zhang J, Liu L, Li J, Liu Z. Effect of raw material ratios on the compressive strength of magnesium potassium phosphate chemically bonded ceramics. Mater Sci Eng C Mater. 2013;33:5058–63.
10. Wu F, Wei J, Guo H, Chen F, Hong H, Liu C. Self-setting bioactive calcium–magnesium phosphate cement with high strength and degradability for bone regeneration. Acta Biomater. 2008;4:1873–84.
11. Demeestere K, Smet E, Van Langenhove H, Galbacs Z. Optimalisation of magnesium ammonium phosphate precipitation and its applicability to the removal of ammonium. Environ Technol. 2011;22:1419–28.
12. Masuda YC, Kugimiya SI, Murai K, Hayashi A, Kato K. Enhancement of activity and stability of the formaldehyde dehydrogenase by immobilizing onto phenyl functionalized mesoporous silica. Colloid Surf B. 2013;101:26–33.
13. Wei L, Ke J, Prasadam I, Miron RJ, Lin S, Xiao Y, Chang J, Wu C, Zhang Y. A comparative study of Sr-incorporated mesoporous bioactive glass scaffolds for regeneration of osteopenic bone defects. Osteoporosis Int. 2014;25:2089–96.
14. Zhang JH, Zhao SC, Zhu YF, Huang YJ, Zhu M, Tao CL, Zhang CQ. Three-dimensional printing of strontium-containing mesoporous bioactive glass scaffolds for bone regeneration. Acta Biomater. 2014;10:2269–81.
15. Wu ZY, Tang TT, Guo H, Tang SC, Niu YF, Zhang J, Zhang WJ, Ma R, Su JC, Liu CS, Wei J. In vitro degradability, bioactivity and cell responses to mesoporous magnesium silicate for the induction of bone regeneration. Colloid Surf B. 2014;120:38–46.
16. Ji JJ, Dong XP, Ma XH, Tang SC, Wu ZY, Xia J, Wang QX, Wang YT, Wei J. Preparation and characterization of bioactive and degradable composites containing ordered mesoporous calcium-magnesium silicate and poly(l-lactide). Appl Surf Sci. 2014;317:1090–9.
17. Wu F, Liu CS, O'Neill B, Wei J, Ngothai Y. Fabrication and properties of porous scaffold of magnesium phosphate/polycaprolactone biocomposite for bone tissue engineering. Appl Surf Sci. 2012;258:7589–95.
18. Liu WJ, Zhai D, Huan ZG, Wu CT, Chang J. Novel tricalcium silicate/magnesium phosphate composite bone cement having high compressive strength, in vitro bioactivity and cytocompatibility. Acta Biomater. 2015;21:217–27.
19. Jia JF, Zhou HJ, Wei J, Jiang X, Hong H, Chen FP, Wei SC. Development of magnesium calcium phosphate biocement for bone regeneration. J R Soc Interface. 2010;7:1171–80.
20. Guo Z, Liu XM, Ma L, Li J, Zhang H, Gao YP. Effects of particle morphology, pore size and surface coating of mesoporous silica on naproxen dissolution rate enhancement. Colloid Surf B. 2013;101:228–35.
21. Li Y, Chen B. Factors that affect the properties of magnesium phosphate cement. Constr Build Mater. 2013;47:977–83.
22. Carey LE, Xu HHK, Simon CG, Takagi S, Chow LC. Premixed rapid-setting calcium phosphate composites for bone repair. Biomaterials. 2005;26:5002–14.
23. Zhao L, Burguer EF, Xu HHK, Amin N, Ryou H, Arola DD. Fatigue and human umbilical cord stem cell seeding characteristics of calcium phosphate-chitosan-biodegradable fiber scaffolds. Biomaterials. 2010;31:840–7.
24. Guo H, Su JC, Wei J, Kong H, Liu CS. Biocompatibility and osteogenicity of degradable Ca-deficient hydroxyapatite scaffolds from calcium phosphate cement for bone tissue engineering. Acta Biomater. 2009;5:268–78.
25. Sariibrahimoglu K, An J, van Oirschot BAJA, Nijhuis AWG, Eman RM, Alblas J, Wolke JGC, van den Beucken JJJP, Leeuwenburgh SCG, Jansen JA. Tuning the degradation rate of calcium phosphate cements by incorporating mixtures of poly-lactic-co-glycolic acid microspheres and glucono-delta-lactone microparticles. Tissue Eng Part A. 2014;20:21–2.
26. Shadanbaz S, Waker J, Woofield TBF, Staiger MP, Dias GJ. Monetite and brushite coated magnesium: in vivo and in vitro models for degradation analysis. J Mater Sci Mater M. 2014;25:173–83.
27. Shepherd JH, Shepherd DV, Best SM. Substituted hydroxyapatites for bone repair. J Mater Sci Mater M. 2012;23:2335–47.
28. Gallego D, Higuita N, Garcia F, Ferrel N, Hansford DJ. Bioactive coatings on Portland cement substrates: surface precipitation of apatite-like crystals. Mater Sci Eng. 2008;28:347–52.
29. Gandolfi MG, Taddei P, Tinti A, Dorigo EDS, Rossi PL. Kinetics of apatite formation on a calcium-silicate cement for root-end filling during ageing in physiological-like phosphate solutions. Clin Oral Invest. 2010;14:659–68.
30. Bao C, Chen W, Weir MD, Thein HW, Xu HHK. Effects of electrospun submicron fibers in calcium phosphate cement scaffold on mechanical properties and osteogenic differentiation of umbilical cord stem cells. Acta Biomater. 2011;7:4037–44.
31. Huang Y, Jin XG, Zhang XL, Sun HL, Tu JW, Tang TT, Chang J, Dai KR. In vitro and in vivo evaluation of akermanite bioceramics for bone regeneration. Biomaterials. 2009;30:5041–8.
32. Neira IS. Kolen'ko YV, Kommareddy KP, Manjubala I, Yoshimur M, Guitián F. Reinforcing of a calcium phosphate cement with hydroxyapatite crystals of various morphologies. ACS Appl Mater Interfaces. 2010;2:3276–84.
33. Wu CT, Chang J, Zhai WY, Ni SY. A novel bioactive porous bredigite ($Ca_7MgSi_4O_{16}$) scaffold with biomimetic apatite layer for bone tissue engineering. J Mater Sci Mater M. 2007;18:857–64.
34. Wu CT, Chang J, Wang JY, Ni SY, Zhai WY. Preparation and characteristics of a calcium magnesium silicate (bredigite) bioactive ceramic. Biomaterials. 2005;26:2925–31.
35. Lu JX, Wei J, Gan Q, Lu X, Hou J, Song WH, Yan YG, Ma J, Guo H, Xiao TQ, Liu CS. Preparation, bioactivity, degradability and primary cell responses to an ordered mesoporous magnesium–calcium silicate. Micropro Mesopor Mat. 2012;163:221–8.